International Journal of Aviation Science and Engineering
e-ISSN: 2715-6958 p-ISSN: 2721-5342

AVIA

Original Article

Effects of Transition Strip on Aerodynamic Yaw Derivatives of MULDICON Wing using an Oscillating Rig at Various Angle of Attack

Bilal Haider*, Shuhaimi Mansor, Shabudin Mat, Wan Zaidi Wan Omar and Nazri Nasir

School of Mechanical Engineering, Faculty of Engineering, Universiti Teknologi Malaysia, Skudai, Johor, 81310 Malaysia.

* Correspondence: bilal03944@gmail.com

Received: 5 March 2024; Accepted: 21 May 2024; Published: 10 June 2024

This paper presents the effects of the passive flow control technique using transition strips on the transient aerodynamic stability derivative measured on the MULDICON AVT251 wing. The experiments were performed at two configurations; clean wing configuration and the transition strips attached to wing leading edge. MULDICON wind tunnel model was designed and fabricated in UTM based on the AVT251 design. The dynamic measurements were carried out in the Universiti Teknologi Malaysia Aerolab wind tunnel for Reynolds number of 0.3×10^6 & 0.475×10^6. MULDICON model was confined to oscillate with a single degree of freedom in yawing motion. The aerodynamic stability derivatives C_{n_β} & C_{n_r} are measured as aerodynamic stiffness and damping by extracting the stiffness and damping of the dynamic oscillating rig system. Springs of different stiffness are used to vary the oscillation frequencies with the reduced frequency range of $0.004 - 0.08$. The unsteady aerodynamics effects are examined for both wing configurations. The angle of attack varies from $\alpha = 0^o$ to 20^o by comparing the transient measurements from the dynamic UTM-LST to the steady-state wind tunnel measurements. The dynamic results indicate that the aerodynamic stiffness derivative is not constant and exceeds the static values and strongly correlates with reduced frequency. The aerodynamic damping derivative is a function of reduced frequency as the damping derivatives become more negative with the increase of the reduced frequency. The amplification factor for the stiffness derivative is above unity which indicates that the steady-state derivative is under-predicted.

Keywords: Dynamic oscillatory rig; aerodynamic derivatives; transition strips

1. Introduction

Several extreme flight conditions at a high angle of attack and a large angular rate will be encountered by the flying vehicle during the flight of the modern UCAV wing configurations. Several factors contribute to the unsteady and highly nonlinear aerodynamics and one of them is associated with the low sweep lambda wing UCAV configurations. The Low sweep lambda wing UCAV configuration aerodynamic studies are of prime interest due to the complex vortex flow topology over the wing surface [1]. The investigation and the estimation of the flow topology and stability of the modern UCAV configuration for medium to higher pitch angle, α persists vital to superior manoeuvrability and performance [2]. The dynamic aerodynamic studies need to be carried out to observe the behaviour of the unsteadiness; this can be done either by wind tunnel experiments or by the CFD simulation.

e-ISSN: 2715-6958 p-ISSN: 2721-5342

Many experiments investigate the static and dynamic testing in the wind tunnel that supports the aircraft designers with reliable steady-state and dynamic test data. The experimental setup data can be used for the flight characteristics such as stability analysis and the verification and validation of the CFD simulations [3].

2. Experimental Procedure

To investigate the effects of transition strips on the transient aerodynamic of a generic lambda wing, a model of generic MULDICON wing of AVT 251 was designed and fabricated in UTM Aerolab. The model has a wingspan of 0.6 meters and consists of three different aerofoils, i.e., supercritical Dornier, NACA 64A010 and NACA 65A410 aerofoils. The basic parameters of the wing are shown in table 1. The steady state yaw moment coefficients are measured for the yaw angle β=±20º for wind speed of U=20 and 30 m/s for the angle of attack, α=0-20º with the help of 6-component external force and moment balance which is capable to log the aerodynamic loads at various wind direction by rotation of the wind tunnel (W/T) model via the turntable that is placed underneath the wind tunnel floor.

Table 1. UTM Aero lab MULDICON model parameters.

Parameters	Details
Leading-edge sweep, $\emptyset_{le}$	53°
Leading-edge sweep, $\emptyset_{te}$	30°
Wingspan, b	0.6 m
Reference chord length, C_{ref}	0.234 m
Reference surface area, S_{ref}	0.1216 m^2
Root chord, C	0.391 m

During the experiment, the model was installed in the 2 x 1.5-meter test section, as shown in figure1. The model was attached to the potentiometer through a strut support system. Experiments were run at the speed speeds of 20 & 30 m/s corresponding to Reynolds number of 0.3 x 10^6 & 0.475 x 10^6, respectively. The experiments were performed in two main phases. The first phase was the experiment without passive flow control technique, namely smooth or clean wing. In contrast, the second experiment was the testing where the transition strip was placed at the leading edge of the wing, and this set of experiment was called a transition wing. The surface roughness and width of this transition strip were 500 microns and 3.5mm, respectively. The unsteady response of the MULDICON wing can be studied experimentally at various pitch angles, α, with the help of a single degree of freedom (pure yaw motion) torsion system, as shown in figure1. The dynamic oscillatory system can find out the transient aerodynamic stability derivatives (C_{n_β}& C_{n_r}) and is mounted under the wind tunnel test section. The wind tunnel model is constrained to rotate at the pivot point to obtain the yaw oscillation motion. The dynamic oscillatory rig facility approach to finding out the dynamic stability derivatives is cost-effective and efficient [14].

The springs of different stiffness are used to vary the oscillation frequency to obtain different yaw damping and stiffness derivatives [15]. The dynamic rig is highly sensitive to transient aerodynamic loads. The estimated specific range of interest for the scaled model oscillation frequency (f_{MO}) is 0.21 - 6.34 Hz and the spring stiffness (Ks) is estimated by equation 1.

$$Ks = \frac{Izz((2\pi f_{MO})^2}{2b^2} \quad (1)$$

 doi: 10.47355/AVIA.V6I1.97

e-ISSN: 2715-6958 p-ISSN: 2721-5342

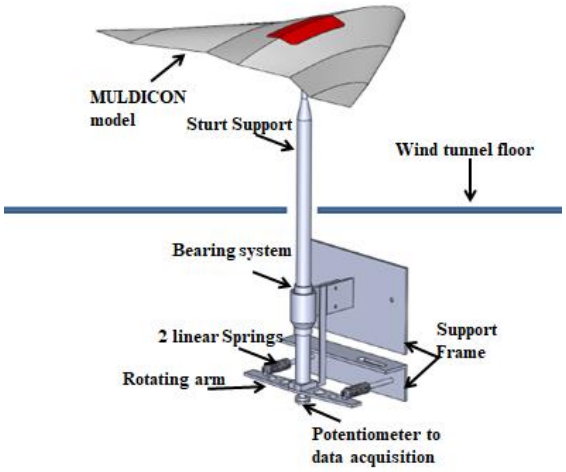

Figure 1. Dynamic oscillatory rig inside the wind tunnel.

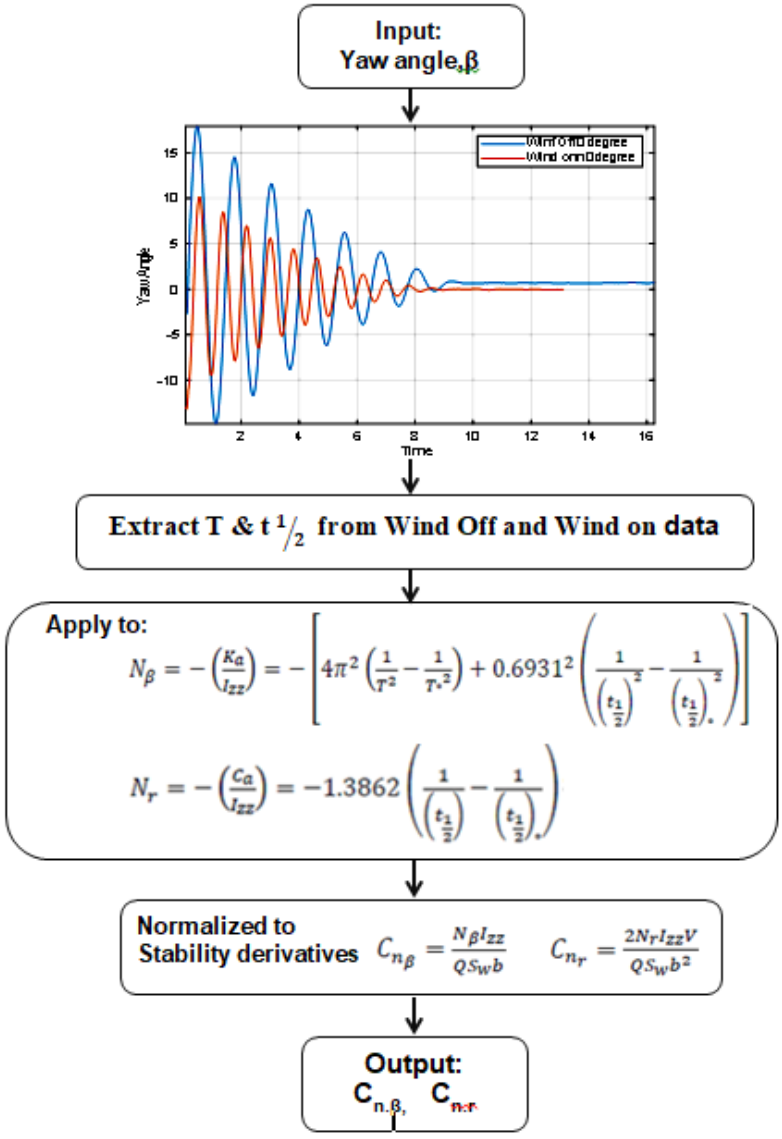

Figure 2. Flow Diagram for dynamic C_{n_β}& C_{n_r}estimation.

e-ISSN: 2715-6958 p-ISSN: 2721-5342

Ks is the spring stiffness, Izz is the moment of inertia, b is the arm length of the dynamic oscillatory rig facility. The springs of the stiffness between 20-1820 N/m are selected, corresponding to the desired reduced frequency range for the dynamic testing of the MULDICON wing. Once the dynamic rig facility is installed, as shown in figure1, the moving arm will be deflected at a positive yaw angle before being released and time histories for the yaw oscillation will be logged. Figure 2 shows the flow of work that will be followed to calculate the dynamic yaw stiffness derivative C_{n_β} and yaw damping derivative C_{n_r}. The reduced frequency is calculated by equation 2, where f is the frequency in Hz is, L is the fuselage length and U is the wind speed in m/s.

$$k_m = \frac{f \times \mathrm{L}}{U} \tag{2}$$

3. Results

Results are attained from the oscillation rig facility with the MULDICON model attached for the workable frequency range = 0.21 - 6.34 Hz that corresponds to the reduced frequency range of 0.004-0.08 specified by the literature [16]. The dynamic stiffness derivatives and the dynamic damping derivatives are reported. The stiffness derivative amplification factor is determined by comparing the dynamic with steady state measured derivatives. The steady state yaw moment coefficients for the clean MULDICON wing and for the configuration with the transition strips attached are shown in figure 3 and figure 4 respectively.

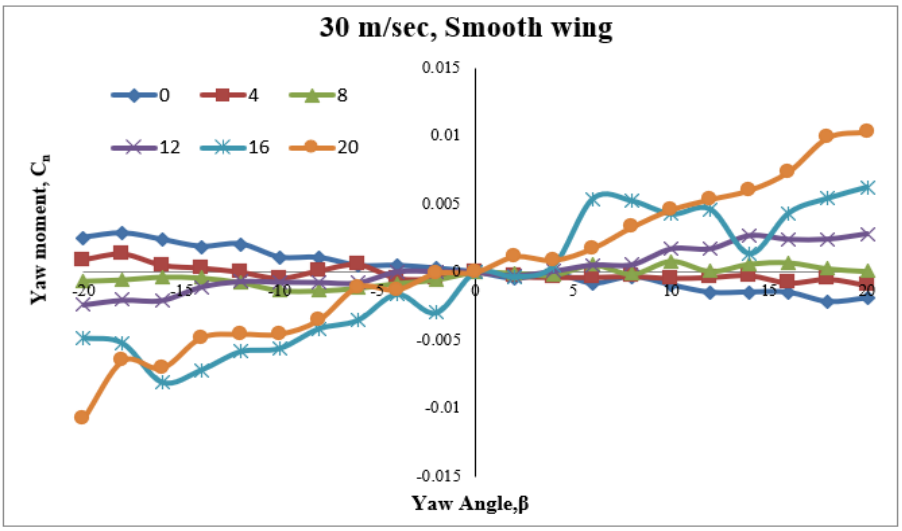

Figure 3. C_n versus β for Clean MULDICON wing.

Figure 5 shows the mass moment of inertia for the wind-off condition for the angle of attack, $\alpha = 0^o$. Comparison of Wind off and Wind on with different wind speeds shows the system is sensitive to aerodynamic damping where the aerodynamic damping increases as the wind speed is increased, as shown in figure 6. Aerodynamic damping also varies with the change in the pitch angle. At lower AOA, aerodynamic damping variation with wind speed is relatively slight as the AOA increases and the aerodynamic damping increases rapidly with the wind speed increase. The effect of aerodynamic damping is visible in figure 6.

 doi: 10.47355/AVIA.V6I1.97

e-ISSN: 2715-6958 p-ISSN: 2721-5342

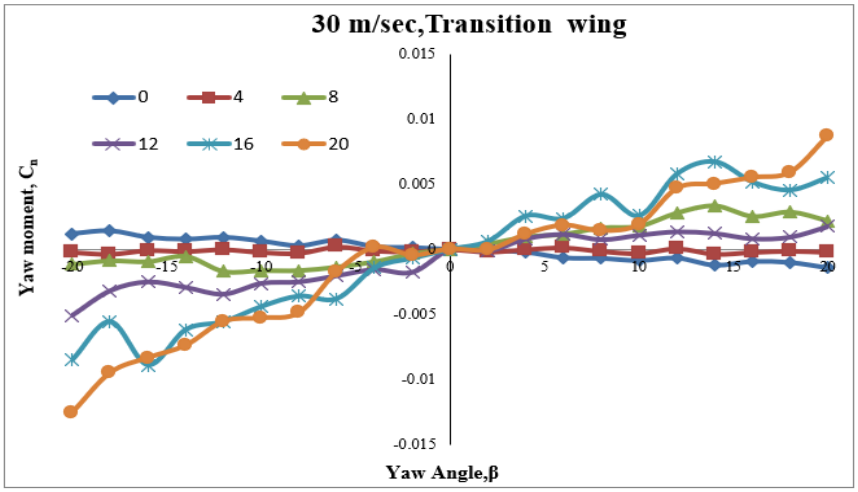

Figure 4. C_n versus β for MULDICON with transition strips attached at leading edge of wing.

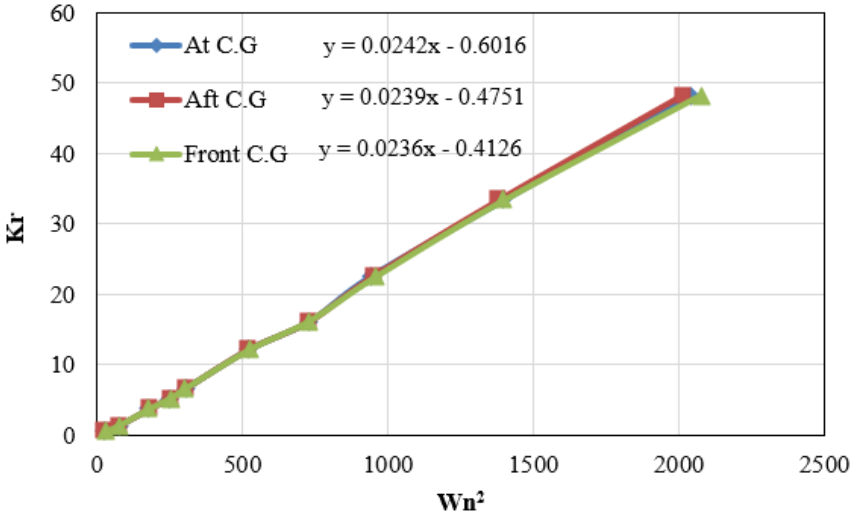

Figure 5. Wind off analysis: Torsional stiffness (Nm/rad) versus square of natural frequency (rad/s) ^{2}

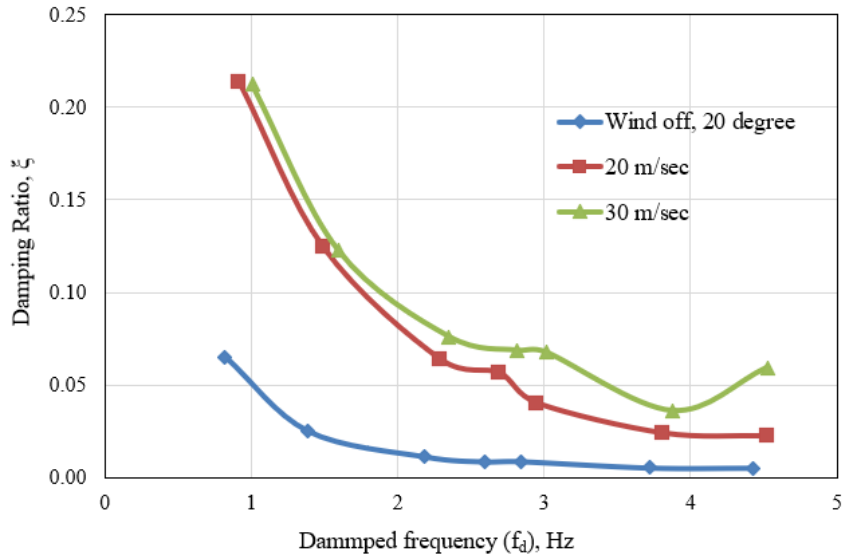

Figure 6. Aerodynamic damping (ξ) versus damped frequency (f_d).

doi: 10.47355/AVIA.V6I1.97

e-ISSN: 2715-6958 p-ISSN: 2721-5342

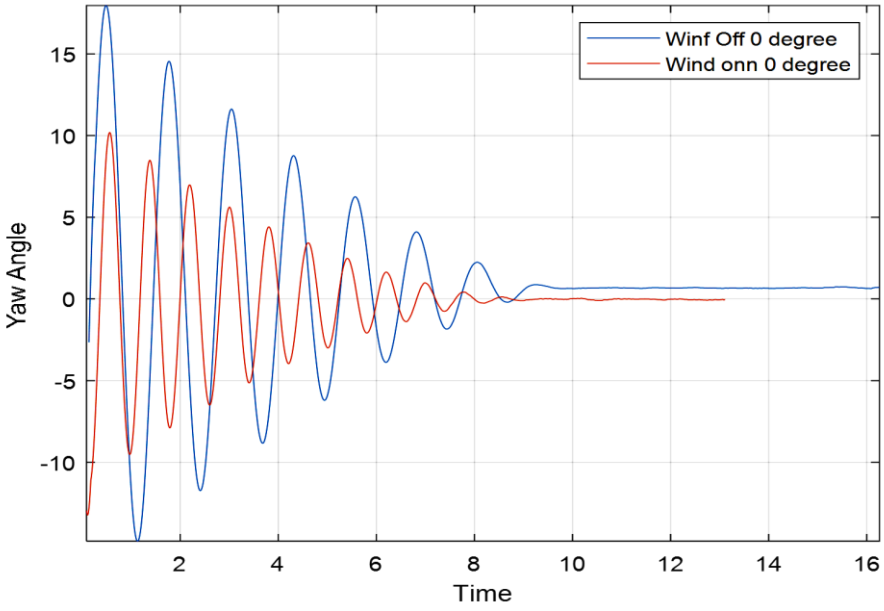

Figure 7. Wind off versus Wind on oscillations for angle of attack = 0°

Comparison of the Clean MULDICON wing configuration with the MULDICON wing configuration with the transition strips attached are given in figure 8. At low reduced frequencies, the aerodynamic stiffness derivative C_{n_β} are less distributed for both configurations for all angle of attack range and the increment the angle of attack leads to higher directional stability for both configurations. The increase in the reduced frequency for the clean MULDICON wing configuration leads to decreased directional stability, whereas the MULDICON wing with the transition strips attached possesses slightly higher directional stability at a higher reduced frequency.

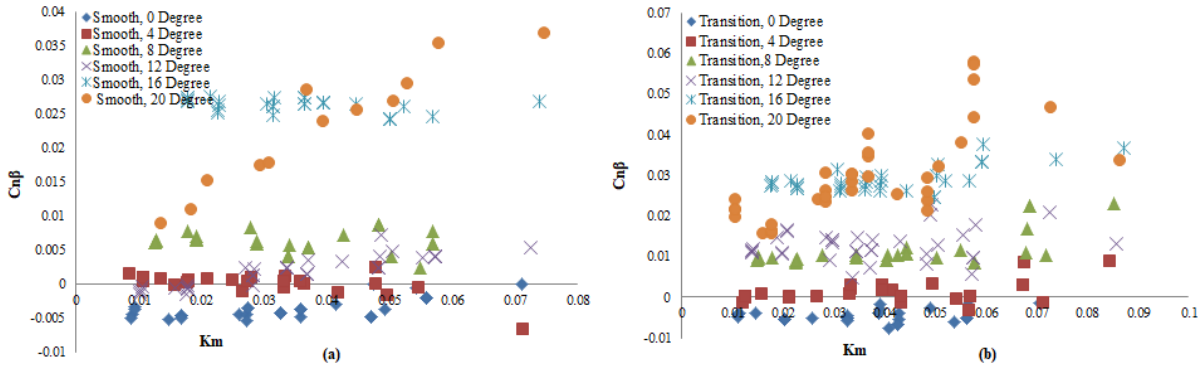

Figure 8. (a) C_{n_β} vs Km, Clean MULDICON wing, (b) C_{n_β} vs Km, MULDICON with transition strips attached.

Figure 9 shows the aerodynamic damping derivative variation with reduced frequency for both MULDICON configurations with and without the transition strips attached for the angle of attack of 0^0,4^0,8^0,12^0,16^0 & 20^0 where at a higher reduced frequency, the aerodynamic damping is more scattered for all angle of the angle of attack. At lower reduced frequency, the aerodynamic damping is more presentable for all ranges of the angle of attack where the yaw damping derivative is increased which indicates that the damping of the aircraft is a function of reduced frequency, and it is not a constant value.

 doi: 10.47355/AVIA.V6I1.97

e-ISSN: 2715-6958 p-ISSN: 2721-5342

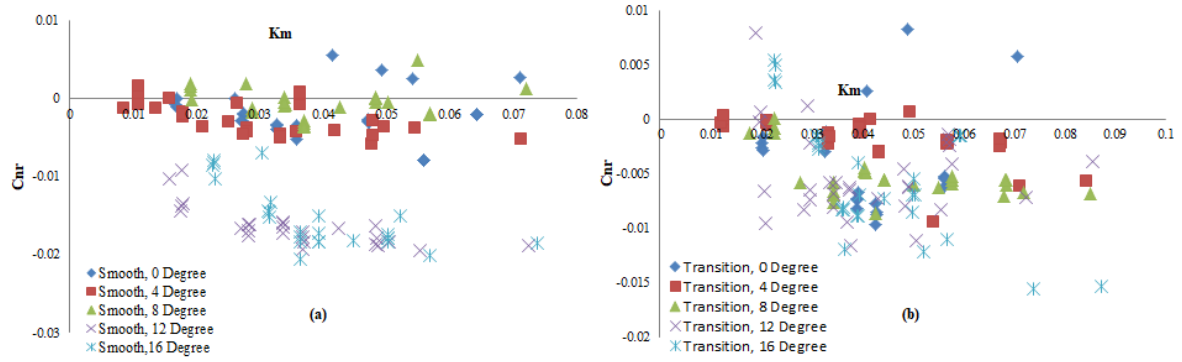

Figure 9. (a) C_{n_r} versus Km, Clean or smooth MULDICON wing, (b) C_{n_r} versus Km, MULDOCON wing with transition strips attached.

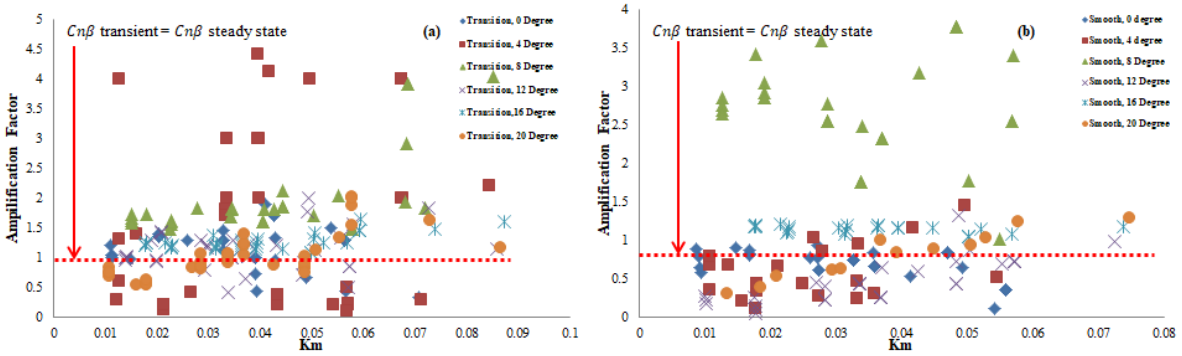

Figure 10. (a) AF(C_{n_β}) vs Km, Clean MULDICON wing, (b) AF(C_{n_β}) vs Km, MULDICON wing with transition strips attached.

The aerodynamic amplification factor AF (C_{n_β})is a ratio between transient and steady-state derivatives measurements. For the most part of the reduced frequency the amplification factor is above unity, as shown in figure 9 which indicates that the estimation of aerodynamic derivatives using steady-state measurement technique is under-predicted hence are not applicable to represent their response, especially in the transient case.

5. Conclusions

The dynamic results indicate that the aerodynamic stiffness derivative is not constant and exceeds the static values and strongly correlates with reduced frequency. The increase in the reduced frequency for the range of angle of attack leads to the decrease in directional stability derivative for the clean MULDICON wing, whereas the directional stability derivative increases for the MULDICON wing with the transition strips attached. The aerodynamic damping derivative is also a function of reduced frequency as the damping derivatives become more negative with the increase of the reduced frequency. For the higher angle of attack, the damping derivative values become more negative, indicating that the damping is increased for the higher angle of attack. Amplification factor for the stiffness derivative is above unity which indicates that the estimation of aerodynamic derivatives using the steady-state measurement technique is not applicable to represent their response, especially in the transient case.

 doi: 10.47355/AVIA.V6I1.97

e-ISSN: 2715-6958 p-ISSN: 2721-5342

Acknowledgments

The experiments have been carried out in UTM Aerolab. The main author acknowledges the Higher Education Commission for funding his Ph.D. study.

References

1. Rockwell, D 1993 Three-dimensional flow structure on delta wings at high angle-of-attack-Experimental concepts and issues. 31st Aerospace sciences meeting.
2. Schütte A, Vormweg J, Maye RG, Jeans T 2018 Aerodynamic shaping design and vortical flow design aspects of a 53deg swept flying wing configuration. Appl. Aerodynamics Conf.
3. Dadkhah M, Masdari M, Vaziri MA 2019 The effects of flow separation on a lambda wing aerodynamics. Aircraft Eng. and Aerospace Tech.
4. Huber KC, Schütte A, Rein M, Löser T 2017 Experimental aerodynamic assessment and evaluation of an agile highly swept aircraft configuration. CEAS Aeronautical J. 8(1): p. 17-29.
5. Jentzsch, MP, Taubert L, Wygnanski IJ 2017 On the Use of Sweeping Jets to Trim and Control a Tailless Aircraft Model 35th AIAA Appl. Aerodynamics Conf.
6. Jentzsch MP, Taubert L, Wygnanski IJ 2016 Active flow control on the stability and control configuration (SACCON). in 8th AIAA Flow Control Conf.
7. Rosenblum, JP, 2016 An overview of flow control activities at Dassault Aviation over the last 25 years. The Aeronautical J. 120(1225): p. 391-414.
8. White FM, Corfield I, 2006 Viscous fluid flow Vol. 3.
9. Luo D, Huang D, Sun X, Passive flow control of a stalled airfoil using a microcylinder J. of Wind Engg. and Industrial Aerodynamics, 2017. 170: p. 256-273.
10. Fatehi M, Ahmadabadi MN, Nematollahi O 2019 Aerodynamic performance improvement of wind turbine blade by cavity shape optimization. Renewable Energy 132: p. 773-785.
11. Bai Yl, Ma X, Ming X 2011 Lift enhancement of airfoil and tip flow control for wind turbine App.Mathematics and Mech. 32(7): p. 825-836.
12. Buzica A, Debschütz L, Knoth F, Breitsamter C 2018 Leading-Edge Roughness Affecting Diamond-Wing Aerodynamic Characteristics. Aerospace 5(3): p. 98.
13. Hövelmann, A, Breitsamter C. 2015 Leading-edge geometry effects on the vortex formation of a diamond-wing configuration. J. of Aircraft 52(5): p. 1596-1610.
14. Rajamurthy M, 1997 Generation of comprehensive longitudinal aerodynamic data using dynamic wind-tunnel simulation. J. of Aircraft 34(1): p. 29-33.
15. Xiqi D, Wei-dong H, Chen B 2006 Summary of the Dynamic Test Capabilities at Caria Low Speed Wind Tunnel. in 25th Int. Congress of the Aeronautical Sciences.
16. Mansor S, Passmore M, 1997 Measurement of a bluff body aerodynamic yaw moment magnification and damping using a dynamic wind tunnel facility. J. of App. Mechanics 78(3).